Fission of drops induced by angular momentum

A. CUEVAS, M. CHAPA, M. SILVA AND A. MENCHACA-ROCHA
Instituto de Física, Universidad Nacional Autónoma de México
Apartado postal 20–364, 01000 México, D.F., México

Recibido el 11 de noviembre de 1992; aceptado el 17 de febrero de 1993

ABSTRACT. The collisions of $m = 0.3$–2.0 g, $v = 5$–50 cm/s, mercury drops are studied experimentally. A transition between a fusion and a fission outcome is observed, and found to be influenced by angular momentum. The mass dependence measured for the limiting angular momentum L_c(ex) is compared with predictions L_c(th) of a surface potential, the *rotating liquid-drop model* widely used in nuclear physics. A systematic $L_c(\text{ex}) \leq L_c(\text{th})$ discrepancy is found in these and in other drop collision data. Dynamical considerations, and the use of more elaborate surface shapes than those assumed by the model are found to reduce the disagreement.

RESUMEN. Las colisiones de gotas de mercurio con masas $m = 0.3$–2.0 g y velocidades $v = 5$–10 cm/s son estudiadas experimentalmente. Se observa que existe un momento angular L_c que determina la transición entre la fusión y la no-fusión de las gotas. La dependencia con la masa del L_c(ex) medido se compara con las predicciones L_c(teo) de un modelo de potencial superficial, comúnmente aplicado en física nuclear. Tanto en nuestros datos como en los de otros autores, se encuentra que L_c(teo) sistemáticamente sobreestima L_c(ex). Se muestra cómo esta discrepancia puede ser disminuida si se toman en cuenta efectos dinámicos, así como formas más elaboradas para representar la superficie de las gotas.

PACS: 47.10.+g; 03.20.+i; 25.70.–z

1. INTRODUCTION

The behavior of liquid drops represents a classical source of scientific inspiration. This interest is partly due to the fact that the scaling properties of fluid systems allow a generalization of certain laws from the largest astronomical objects to the nuclear [1], and even sub-nuclear [2], level. One such law states that there is a limiting angular momentum L_c that a rotating drop can stand before it disintegrates, typically, into two smaller pieces [3]. Assuming that the conditions leading to such "fissioning" result from the dominance of the repulsive centrifugal (plus Coulomb, for charged drops, or atomic nuclei) force over the attraction due to surface tension (plus gravitation, for astronomical objects), Cohen, Plasil and Swiatecki [4] (CPS), developed a scheme to estimate L_c, and its dependence on the drops' mass. To test this *rotating liquid-drop model* (RLDM) limit it would be neccesary to induce a variable angular momentum on isolated drops of different masses. These experimental conditions, difficult to meet for macroscopic drops in an earthly laboratory [5] are characteristic of atomic nuclei. Thus, since the nucleus behaves collectivelly as a fluid, it is not surprising that the RLDM has been most extensively used in nuclear physics where, among other applications, it has helped in understanding the difficulties encountered in the systesis of heavy elements [6]. In general terms, however, the

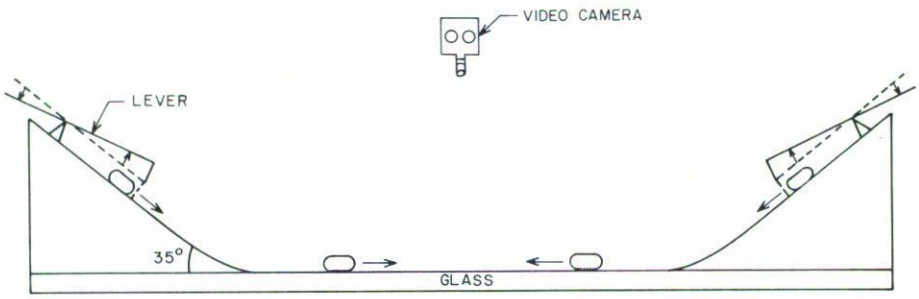

FIGURE 1. Schematic view of the "gotatron".

need to include a number of corrections characteristic of nuclear systems (finite range [7] and diffusse potentials [8], detailed structure effects [6], etc.) indicate that the nucleus may not be the best ground to test the "bare" RLDM and, in particular, its prediction for the mass dependence of L_c.

Concerning macroscopic systems, the Spacelab experiments [5] on the behavior of drops spinning in a microgravity enviroment demonstrated the existence of a critical rotational velocity. As in nuclear reactions, angular momentum limitations also affect the probability of coalescence for small drops. This is relevant, for example, in the understanding of atmospheric phenomena [9] as well as in the development of liquid sprays [10]. Indeed, the existence of rotational instabilities has been stablished while studying the collisions of small drops [11, 12]. However, none of those studies [5, 11, 12] has been directly concerned with determining L_c values. Still, given its extensive applicability in other fields, it would seem reasonable that the $L_c(m)$ predictions of the RLDM be tested on... drops.

Here we report an experiment designed to study the mass dependence of the limiting angular momentum for the coalescence, or "fusion", of liquid-drops. A brief account of our results, not including the experimental details and part of the analysis, has been presented elsewhere [13].

2. MEASUREMENTS

The measurements were carried out with the aid of a liquid-drop collider, the "gotatron", in which we observe the interactions of equal size mercury drops moving along a flat, horizontal, glass surface, specially treated [14] to minimize the drag induced by wetting.

Two drops, each of mass m, are "accelerated" to equal and opposite, velocities v, with the aid of plastic ramps fixed on two extremes of the glass surface (Fig. 1). A groove on each ramp surface guides the drops down the slopes and smoothly into parallel trajectories separated by an impact parameter b. In this way, the outcome of the drop collisions can

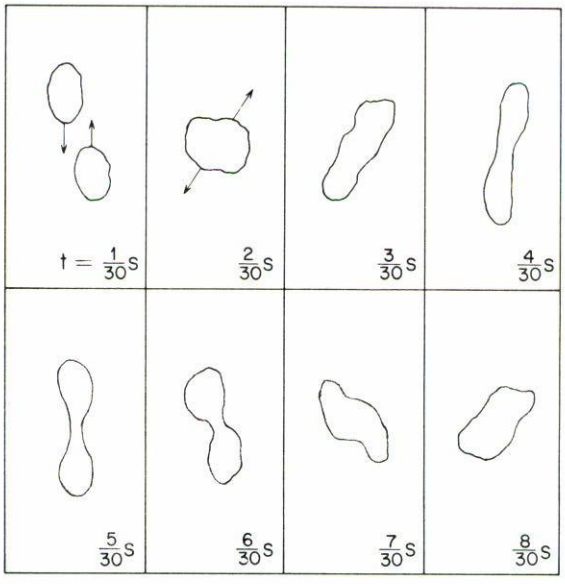

FIGURE 2. Time evolution a fusion drop-drop collision measured for a symmetric $m = 1$ g system. The arrows in the initial (top left) frame indicate the original direction of motion. The arrows in the 2nd frame point at the "side splash" of matter in the contact region.

be studied as a function of b, $|v|$ and m. The possition *vs.* time information needed to determine v and b is obtained by recording the action with a fast-shutter-speed (1/4000 s) video system having a 30 frames/s recording frequency. The drop initial masses m are measured with a 0.1 mg precision analytic scale. For technical reasons [14], the gotatron is limited to observe the collisions of mercury drops having masses and velocities in the range 0.2 g $\leq m \leq$ 2.0 g, and 5 cm/s $\leq |v| \leq$ 50 cm/s, respectively. The action of every drop collision experiment lasts, typically, 1 s (*i.e.* 30 frames). The image information on each frame consists on 620,000 color pixels. For simplicity, in the present study this volume of information was reduced to the drop contours on each frame, using standard image processing techniques. Figures 2 and 3 show examples of typical sequences of 8 frames taken during a fusion and a non-fusion collision, respectively. More details about the drop "acceleration" procedure used may be found in Ref. [14]. First we show that, in the gotatron, the drop-glass interaction is small when compared with the drop-drop interactions. For this purpose, let us considere an "inelastic" drop-drop collision; *i.e.*, one ending in a two-drop state in which the final drop masses are very similar to the initial ones (as in Fig. 3). This interactions favour our comparison since in them the amount of relative energy lost to internal degrees of freedom is small, compared with fusion events, where all the relative energy is lost that way. Figure 4 shows a typical example of the time evolution of the total kinetic energy $E_{\mathrm{T}}(t)$ (*i.e.*, the sum of the individual kinetic energies) of drop pairs having $m = 1$ g. There are three distinct regions in the resulting $E_{\mathrm{T}}(t)$ curve: I) before, II) during, and III) after the collision. Extrapolating the strenght of the drop-glass interaction from region (I), we find that the rate of kinetic energy loss

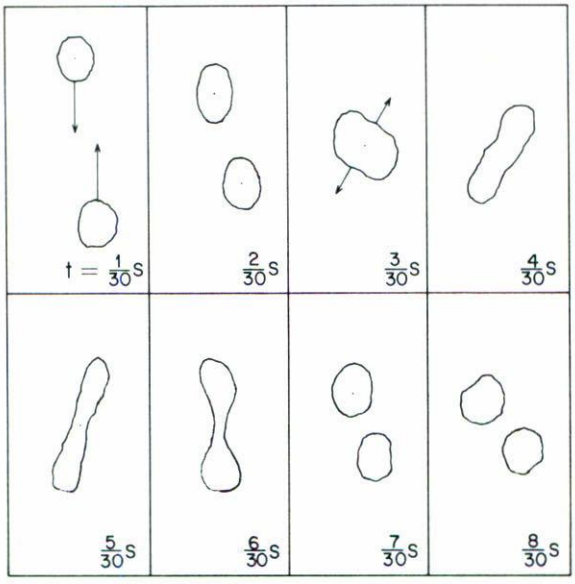

FIGURE 3. Time evolution of an "inelastic" drop-drop collision measured for a symmetric $m = 1$ g system. The arrows in the initial frame have the same meaning as in Fig. 2. The arrows in the 3rd frame point at the "side splash" of matter in the contact region.

during the collision is, at least, an order of magnitude greater than before, or after, the drop-drop contact.

With this experimental setup, we have investigated the influence of angular momentum L on the probability for fusion for 8 different symmetric systems of total masses $M = 2m = 0.6$, 1.0, 1.6, 2.0, 2.6, 3.0, 3.6 and 4.0 g. For each M value, 24 collisions were recorded for a set of pre-established values of $|v|$ and b based on our calibration of the apparatus. However, to calculate L, the actual values of v and b that the drops have upon contact were extracted from a frame-by-frame analysis of the position of each drop. In this way, a binary variable $N(L)$ was assigned to the outcome of every collision, which distinguished between a "fusion", $N = 1$, event (only one drop in the final channel) from a "nonfusion", $N = 2$, (two or more drops) event. Figure 5 shows an example of the results, obtained for $M = 2$ g, in which a fusion-nonfusion transition is observed. A "critical" value, L_c, was extracted by a $N(L) = 2 - (1 + \exp((L - L_c)/R))^{-1}$ fit, leaving L_c and R as free parameters. The width of the transition region, measured by the parameter R, is partly due to oscillations induced on the drops by the acceleration procedure (see initial frames in Figs. 2 and 3). Since these shape perturbations have an arbitrary phase relative to the contact time, they broaden the L distribution, increasing the uncertainty in the determination of L_c. The error-bar associated to each L_c, which reflects this effect, was taken to be 4.4 R, which is the width of the $1.1 \leq N \leq 1.9$ region. As can be appreciated (Fig. 5), outside this relatively narrow transition zone, L is a determining factor for the outcome of the collisions. The resulting L_c values are given in Table I and ploted as a function of M in Fig. 6.

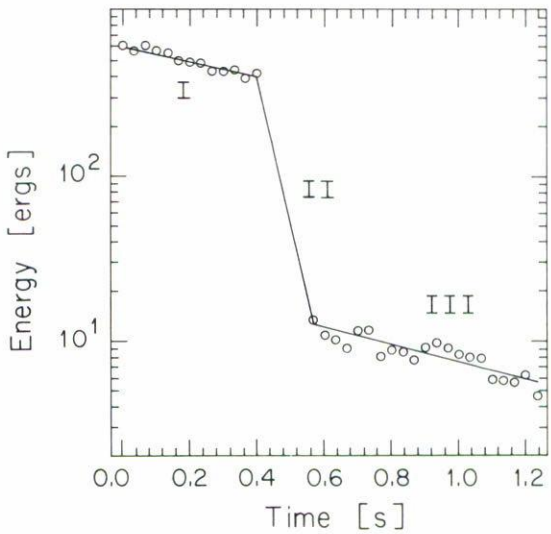

FIGURE 4. Evolution of the total energy measured (dots) before (I) and after (III) an inelastic drop-drop encounter. The lines represent the best fit of an $E(t) = \frac{1}{2}\mu V_0^2 \exp[(-(2\beta_i/\mu)t]$ parametrization which assumes the action of a velocity dependent friction force (see Ref. [14]), where V_0 is the initial velocity, μ is the reduced mass, and β_i is the friction parameter. The rate of energy loss during the collision (II) was estimated by joining curves I and III, using the same parametrization. The friction coefficients used to draw the lines were $\beta_{\rm I} = 0.5$ g/s, $\beta_{\rm II} = 13.6$ g/s, and $\beta_{\rm III} = 0.6$ g/s.

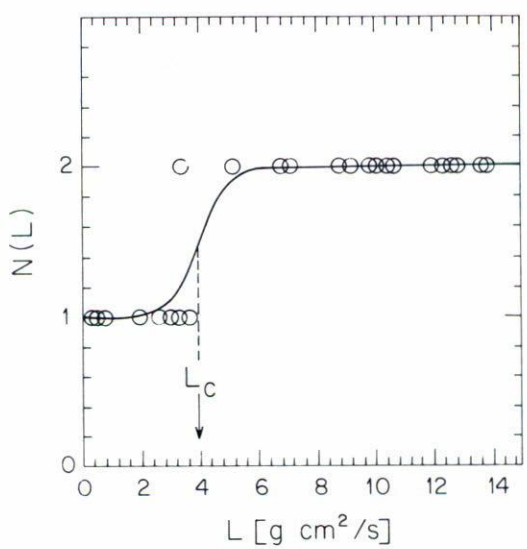

FIGURE 5. The outcome $N(L)$ observed for symmetric $m = 2$ g drops as a function of angular momentum L. The $N = 1, 2$ circles represent fusion and non-fusion events, respectively. The curve represents a fit (see text) used to determine the limiting angular momentum L_c.

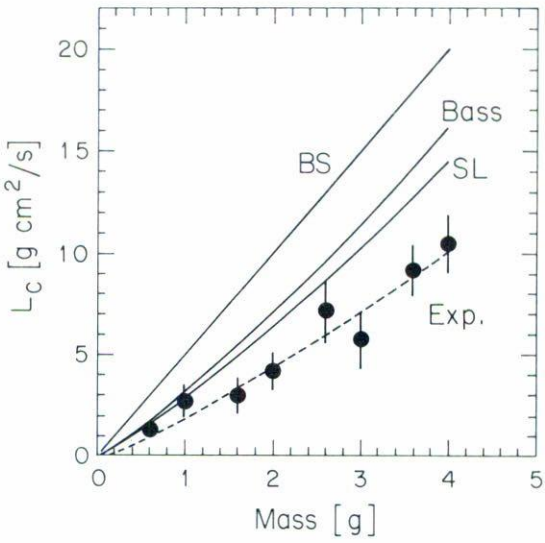

FIGURE 6. Measured limit of angular momentum for the fusion of mercury drops as a function of mass (circles). The dashed curve was drawn to guide the eye. The BS curve represents the gyrostatic RLDM predictions using the BS code [15] for spherical drops. Our estimate for the effect of an oblate deformation yields results which are indistiguishable from this curve. The Bass curve represent the predictions of the Bass model [22]. The SL curve results from imposing the condition proposed by Schmidt and Lutz [25] on the potential surface predicted by the BS model [15].

3. DISCUSSION

The observed near-linear dependence of L_c on the drops' mass is reminiscent of the CPS predictions for light nuclei [4], in the region where Coulomb effects are small. As mentioned before, acording to the RLDM [4], the $L_c(m)$ behavior results from the a balance between the surface tension and the repulsive forces acting. The calculations of L_c take into account the fact that the shape of the two-drop system evolves as a function of their separation (ρ). For example, in their RLDM calculations Cohen, Plasil and Swiatecki [4] solve the equations of motion of two rotating spheres connected by a conical neck. In a more sophisticated RLDM estimate, Blocki and Swiatecki [15] (BS) represent the neck by a quadratic surface of revolution characterized by a neck-size parameter λ. Ignoring dynamical effects, the λ–ρ potential energy surfaces can be used to estimate L_c by searching the L value for which the potential energy hollow disapears. The solid line Fig. 6 represents the predictions of such BS model estimates for equal, spherical and electrically neutral mercury drops. As can be seen, these RLDM calculations reproduce the near-linear mass dependence but overestimate L_c by a factor of ≈ 2. We now investigate some of the possible reasons for this large discrepancy.

First, an experimental aspect to be considered is the fact that mercury drops lying on a horizontal glass surface assume shapes which are closer to oblate spheroids than to spheres. Although a generalization of the surface potential models to spheroidal shapes is beyond the scope of our work, the systematics of the BS calculations indicate a simple way to estimate the influence of an oblate-spheroidal deformation on $L_c(m)$. Within the L-value

range of interest here (Fig. 6), the BS model predicts that the saddle-point in the ρ–λ potential surface (which determines the fusion-nonfusion transition) remains at an approximatedly fixed possition (ρ_c, λ_c). Furthermore, the calculations indicate that this critical point lies close to the two-separate-drop shape limit. Thus we have developed a simplified model in which the surface of the system is estimated by two spheres separated by a variable distance parameter ρ, joined by a quadratic-shape neck having the characteristic dimension $\lambda = \lambda_c$ at $\rho = \rho_c$. The $L_c(m)$ predictions of this "uni-dimensional" potential (using the hollow-dispearence criterium) coincide with those of the two-dimentional BS calculation for spherical drops [15]. The simplified surface model was, then, modified to take into account an oblate drop deformation, using the observed experimental shapes [14] to determine the spheroid parameters. The L_c values predicted this way are only $\approx 1\%$ smaller than those predicted by the BS for spherical drops. This insensitivity of the predictions to the shape changes is due to the near cancellation between two opposite effects. First, compared with the spherical case, the deformed drops are subject to a less attractive surface potential, what has the effect of decreasing L_c. However, the oblate deformation involved here implies an increment in the drop dimensions along the contact plane. Hence, relative to the spherical case, the drops touch at a larger distance, where the centrifugal force has smaller values, having the effect of increasing L_c. The same deformation insensitivity is found if the effect of deformation is simulated on the BS calculation for spheres by decreasing the potential depth, and increasing the radial dimensions, for each mass, through equivalent reductions in the surface tension and in the density. Thus, we are lead to conclude that this type of deformation may not be the main source for the large discrepancy shown in Fig. 6 between theory and experiment.

Another experimental effect which, at first sight, might influence our L_c measurements is the angular momentum associated to the fact that the mercury drops are *rolling* [14] (rather than sliding) along the glass surface. Note, however, that these angular momentum components are perpendicular to the angular momentum involved in the collision.

As mentioned in the introduction, there are independent evidences for a systematic overestimation of L_c by the BS gyrostatic model predictions for drops. We have analysed the data from Adam, Lindblad and Hendricks [11] for spherical, electrically charged, water drops of $m = 0.9$ and 113 μg and from Brenn and Frohn [12] for spherical, uncharged, propanol-2 drops of $m = 0.15, 0.4, 1.7$ and 3.3 μg. These authors [11, 12] studied the fusion-nonfusion transition on collisions of equal-size drop, as a function of the relative velocity v_r and impact parameter, b. A typical example [11] of these type of data is shown in Fig. 7.

According to Natowitz and Namboodiri [16], and to Griffin and Wong [17], the transition observed in Fig. 7 is due to two independent effects: rotational instabilities, pressumably related to L_c, and vibrational instabilities. The latter were introduced to explain the back-bend in the fusion-nonfusion transition observed in the water data [11] at small impact parameters (see Fig. 7). No back-bend is observed in the propanol-2 data of Ref. [12], pressumably due to the fact that no small impact parameter measurements are reported. Thus, excluding the b, v_r pairs in the back-bend region for water drops, we have used the rest of the water data [11], and all of the propanol-2 data [12], to extract average L_c values by fitting a $b = 2L_c/mv_r$ relationship. The experimental results (L_c(ex)) are included in Table I, together with the corresponding predictions L_c(th) from the BS

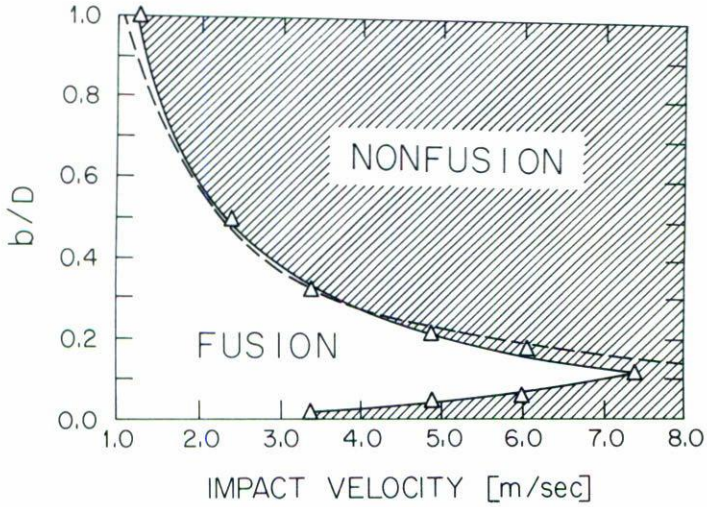

FIGURE 7. The fusion-nonfusion transition, as a function of impact parameter (normalized by the drops' diameter D) and relative velocity, measured (solid curve) by Adam, Lindblad and Hendricks [11] on $m = 113$ μg diameter water drops. The solid curve, drawn [11] to gide the eye, marks the separation between fusion and nonfusion collisions. The dashed curve is the result of a $b = 2L_c/mv_r$ fit used to extract the average values of L_c.

model for spherical (and, when appropiate [11], charged) drops. The quoted uncertainties are equal to the standard deviation of the L_c's, obtained from each b, v_r pair, relative to the mean. The values of surface tensions and densities used are indicated in the table caption. The right column shows the ratio between the experimental and the theoretical L_c values, illustrating that the magnitude of systematic deviation is similar to what we found for mercury drops. This fact supports our arguments for neglecting the experimental effects associated to the oblate deformation and rolling motion of the mercury drops.

A common feature of the data shown in Table I is that the corresponding experiments were carried out under the action of a small external (drop-glass and/or aerodynamic) retarding force. However, this implies that, for a fixed impact parameter, the initial velocities need to be incremented accordingly to obtain the same outcome, indicating that the discrepancy with the RLDM estimates may be even larger.

There are several theoretical aspects which could help explain the discrepancy between the RLDM estimates and the drop collision measurements. One of them is the need for dynamical (viscous friction, shape evolution, etc.) effects. This deficiency of gyrostatic RLDM [4] calculations is well known in nuclear physics [18]. A macroscopic approach [19] to solve this problem has been to assume a friction mechanism and then to solve the dynamical ecuations following the time evolution of the nuclear collisions. That procedure systematically yields lower fission barriers and, thus, predict smaller L_c values. However, those calculations [19] would be difficult to addapt to macroscopic fluids astheir dynamics are based on a *one-body* dissipation mechanism which is characteristic of nuclear reactions at low incident energies [20]. Ordinary fluids and high energy nuclear reactions

TABLE I. Limiting angular momenta extracted from the present mercury-drop data, as well as from the available water [11] and propanol-2 [12] data. The liquid densities (ρ_l, in g/cm^3) and surface tensions (σ in dynas/cm) assumed in these calculations were: $\rho_l = 13.0$, $\sigma = 435.0$ for Hg; $\rho_l = 1.0$, $\sigma = 73.5$ for H_2O; and $\rho_l = 0.78$, $\sigma = 21.4$ for propanol-2.

Liquid	M [g]	V_r [cm/s]	L_c(ex) [g cm^2/s]	L_c(th) [g cm^2/s]	L_c(ex)/L_c(th)
Hg	0.6	5–50	1.3 ± 19 %	2.23	$0.58 \pm .11$
Hg	1.0	5–50	2.7 ± 29 %	4.05	$0.67 \pm .19$
Hg	1.6	5–50	3.0 ± 22 %	7.01	$0.43 \pm .09$
Hg	2.0	5–50	4.2 ± 24 %	9.09	$0.46 \pm .11$
Hg	2.6	5–50	7.2 ± 21 %	13.35	$0.58 \pm .12$
Hg	3.0	5–50	5.8 ± 28 %	14.59	$0.40 \pm .11$
Hg	3.6	5–50	9.2 ± 14 %	18.50	$0.51 \pm .07$
Hg	4.0	5–50	10.5 ± 14 %	20.42	$0.51 \pm .07$
Water	1.8×10^{-6}	220–800	$9.5 \times 10^{-7} \pm 31\%$	1.8×10^{-6}	$0.53 \pm .16$
Water	2.2×10^{-4}	120–740	$3.6 \times 10^{-4} \pm 13\%$	5.0×10^{-4}	$0.72 \pm .09$
Propanol-2	3.1×10^{-7}	270–905	$1.0 \times 10^{-7} \pm 30\%$	1.5×10^{-7}	$0.70 \pm .21$
Propanol-2	8.2×10^{-7}	340–845	$2.4 \times 10^{-7} \pm 34\%$	4.7×10^{-7}	$0.51 \pm .17$
Propanol-2	3.4×10^{-6}	425–910	$1.0 \times 10^{-6} \pm 40\%$	2.2×10^{-6}	$0.47 \pm .19$
Propanol-2	6.3×10^{-6}	400–500	$2.5 \times 10^{-6} \pm 18\%$	5.3×10^{-6}	$0.48 \pm .09$

are affected by a *two-body* viscosity [21]. Still, the reducing effect on L_c due to dynamics can be illustrated (Bass curve in Fig. 6) by the use of a simple model proposed by R. Bass [22] in which a uni-dimensional potential is combined with a sharply localized friction approximation.

A deficiency of the BS [15] potential energy surface calculations is that, when applied to drops, the two-dimensional shapes are inadecuate to describe the evolution of the collisions, particularly in their initial stages. This is illustrated in Figs. 2 and 3 showing a side-splash, characteristic of colliding hydrodynamical systems [23], occurring in the contact region (see 3rd frames in Figs. 2 and 3). Note that the intersecting-spheres configurations, which would contain the splash shapes, are especifically excluded in the λ–ρ potential energy surfaces in the BS [15] calculations. Acording to Blocki [24], to introduce those feature in that formalism would require, at least, a fit to the surface shape with a polinomial of a higher order than the quadratic currently used to represent the "neck" degree of freedom. In general, however, the complex shapes adopted by colliding drops would require the use of a multidimensional surface potential. Schmidt and Lutz [25] recently proposed that the effect of those complex deformations on L_c can be estimated using a *shallow potential* approximation, in which the limiting L would be reached when the fission barrier measured at the saddle point equals the total collective energy of the spherical complex. This two-point calculation yields L_c estimates (curve labeled SL in Fig. 6) which are systematically 30% smaller than those predicted by the pocket-dissapearing condition in the surface potential calculations [4, 15]

4. CONCLUSIONS

The above arguments indicate that when considered separatly, both the dynamical aspects and the more complex surface shapes are expected to have important reducing effects on the L_c predictions. It would be interesting to perform two-body-friction dynamical calculations, of the type performed for nuclei by Davies, Sierk and Nix [21], or the full hydrodynamical calculations as those of Stocker and Greiner [23], to compare with the experimental results presented here. Considering the possible consequences of our observations to the nuclear case, since the splash-like deformations are the external (shape) signs of the response of a (two-body) viscous fluid to incompressibility, we believe that more complicated shapes in dynamical potential energy surface calculations [19] would be necessary, at least, in the incident energy domain where the two-body friction dominantes [20].

We have studied the mass dependence of the limiting angular momentum L_c for the fusion of 0.3 g $\leq m \leq$ 2.0 g mercury drops moving on a rough glass surface which minimizes the effect of wetting. When compared with the predictions of gyrostatic calculations using the model of Blocki and Swiatecki [15], the experimental L_c values are found to be systematically smaller that the predictions. This discrepancy holds for L_c values extracted from available data on water and propanol-2 drop collisions. As in nuclear physics, this overestimation of L_c is an indication of the need for dynamical considerations and, in the particular case of drops, of the need to considere more complex surface shapes.

ACKNOWLEDGEMENTS

We thank Profs. J. Blocki and W.J. Swiatecki for allowing us the use of their surface potential code and for fruitful discussions.

REFERENCES

1. W.J. Swiatecki, "The rotating charged or gravitating liquid drop and problems in nuclear physics and astronomy", in *Proceedings of the International Colloquium on Drops and Bubbles*, edited by D.J. Collins, M.S. Plesset and M.M. Saffren, Jet Propulsion Laboratory, Pasadena, California (1974).
2. E.g., A.P. Vischer, P.J. Siemens and A.J. Sierk, *Z. Phys.* **A340** (1991) 315.
3. R.A. Brown and L.E. Scriven, *Proc. R. Soc. Lond.* **A371** (1980) 331.
4. S. Cohen, F. Plasil and W.J. Swiatecki, *Ann. of Ph.* **82** (1974) 557.
5. T.G. Wang, E.H. Trinh, A.P. Croonquist and D.D. Elleman, *Phys. Rev. Lett.* **56** (1986) 452.
6. K.H. Schmidt and W. Morawek, *Rep. Prog. Phys.* **54** (1991) 949; and references therein.
7. H.J. Krappe, J.R. Nix, and A.J. Sierk, *Phys. Rev. Lett.* **42** (1979) 215.
8. K.T.R. Davies and J.R. Nix, *Phys. Rev.* **C14** (1976) 1977.
9. H.R. Pruppacher and J.D. Klett, *Microphysics of Clouds and Precipitation*, D. Reidel Publ. Co. Dordrect, Holland (1978); and references therein.
10. P. Meakin, *Rep. Prog. Phys.* **55** (1992) 157; and references therein.
11. J.R. Adam, N.R. Lindblad, and C.D. Hendricks, *J. App. Ph.* **39** (1968) 5173.
12. G. Brenn and A. Frohn, *Exp. in Fluids* **7** (1989) 441.
13. A. Menchaca-Rocha, A. Cuevas, M. Chapa and M. Silva, *Phys. Rev.* **E47** (1993) 1433.

14. A. Menchaca-Rocha, *J. Colloid Interface Sci.* **149** (1992) 472.
15. J. Blocki and W.J. Swiatecki, L.B.L. preprint, 12811-UC-34d, May 1982, unpublished.
16. J.B. Natowitz and M.N. Namboodiri, *Phys. Rev.* **C12** (1975) 1678.
17. J.J. Griffin and C.-Y. Wong, "Vibrational Instability: a Possible Test of Nuclear Hydrodynamics", in *Proceedings of the XIV International Winter Meeting on Nuclear Physics*, Bormio, Italy, 1976, 366 pp.
18. J.R. Birkelund and J.R Huizenga, *Ann. Rev. Nucl. Part. Sci.* **33** (1983) 323.
19. S. Bjornholn and W.J. Swiatecki, *Nucl. Phys.* **A329** (1982) 471.
20. F. Gregoire and F. Scheuter, *Phys. Lett.* **146B** (1984) 21.
21. K.T.R. Davies, A.J. Sierk and J.R. Nix, *Phys. Rev.* **C13** (1976) 2385.
22. R. Bass, *Phys. Lett.* **47B** (1973) 139; R. Bass, *Nucl. Phys.* **A231** (1974) 45.
23. H. Stocker and W. Greiner, *Phys. Rep.* **137** (1986) 277; and references therein.
24. J. Blocki, private communication.
25. R. Schmidt and H.O. Lutz, *Phys. Rev.* **A45** (1992) 7981.